The Interfacial Modification of Rice Straw Fiber Reinforced Poly(butylene succinate) Composites: Effect of Aminosilane with Different Alkoxy Groups

Yang Zhao,[1] Jianhui Qiu,[1] Huixia Feng,[2] Min Zhang[3]

[1]*Department of Machine Intelligence and Systems Engineering, Faculty of Systems Engineering, Akita Prefectural University, Akita 015-0055, Japan*
[2]*Department of Petrochemical Technology, Lanzhou University of Technology, Lanzhou 730050, People's Republic of China*
[3]*Department of Chemistry and Chemical Engineering, Key laboratory of Auxiliary Chemistry and Technology for Chemical Industry, Ministry of Education, Shaanxi University of Science and Technology, Xi'an Shaanxi 710021, People's Republic of China*

Received 7 September 2011; accepted 16 November 2011
DOI 10.1002/app.36502
Published online 1 February 2012 in Wiley Online Library (wileyonlinelibrary.com).

ABSTRACT: The effect of aminosilane on the properties of rice straw fiber (RSF) reinforced poly(butylene succinate) (PBS) composites was studied. RSF was pretreated with four different aminosilane coupling agents, 3-aminopropyltriethoxysilane (APTES), 3-aminopropyltrimethoxysilane (APTMES), 3-(2-aminoethylaminopropyl)triethoxysilane (AEAPTES), and 3-(2-aminoethylaminopropyl)-trimethoxysilane (AEAPTMES). The results of Fourier transform infrared spectroscopy (FTIR) and ζ potential measurements confirmed that amino groups were introduced to the silane-treated RSF (TRSF) for all four silane coupling agents. The results also indicated a higher degree of hydroxyl ion adsorption by the fiber surface, which was chemically grafted by silane hydroxyl, was obtained with ethoxy silane than with methoxy silane. This difference might be because the relative rates of hydrolysis and ensuing silanol self-condensation of methoxy silane were too fast to reduce the number of silanol groups grafted on the fiber surface. The TRSF composite produced clearly enhanced tensile properties for the aminosilane coupling agents having ethoxy groups. The AEAPTES-RSF-PBS composite showed the highest tensile strength. It might be because of the higher amino content of AEAPTES than APTES; the amino groups on the surface of TRSF were confirmed by FT-IR to react with the carbonyl groups of PBS to form a blue-shifted hydrogen bond. The water absorption process of composites was found to follow the kinetics and mechanisms described by Fick's theory. The aminosilane treatment significantly reduced the moisture diffusion coefficient but did not change the mechanism of water adsorption. J Appl Polym Sci 125: 3211–3220, 2012

Key words: natural fiber composites; poly(butylene succinate); rice straw fiber; aminosilane; blue-shifted hydrogen bond; moisture diffusion coefficient

INTRODUCTION

Recently, natural fibers such as wood, bamboo, cotton, jute, nut shells, and straw which are used to fill and reinforce thermoplastic matrices have attracted substantial attention because their composites are claimed to offer advantages such as low cost, low density, lower pollutant emissions, lower greenhouse gas emissions, and reducing dependence on nonrenewable energy and material source.[1] Such desirable environmental performance is an important driver for the increased future use of natural fiber composites. Development of commercially viable "natural plastic products" based on natural fiber and biodegradable plastic for a wide range of applications is on the rise.[2–8]

However, the poor interfacial adhesion between natural fibers and thermoplastic matrices prevents widely use of natural fiber composites. The usual hydrophilic fibers have inherently lower compatibility with hydrophobic polymer matrices, and this incompatibility may cause problems in composite processing and in composite material properties. Hydrogen bonds may form between the hydrophilic fibers, and the fibers tend to agglomerate into bundles and unevenly distribute throughout the hydrophobic polymer matrix during processing.[9,10] The moisture absorption of the natural fibers may cause dimensional changes of the resulting composites and weaken the interfacial adhesion.[11,12]

Therefore, surface treatment of natural fibers is beneficial in order to promote interfacial adhesion and improve the water resistance. A coupling agent functions at the interface to create a chemical bridge

Correspondence to: J. Qiu (qiu@akita-pu.ac.jp).

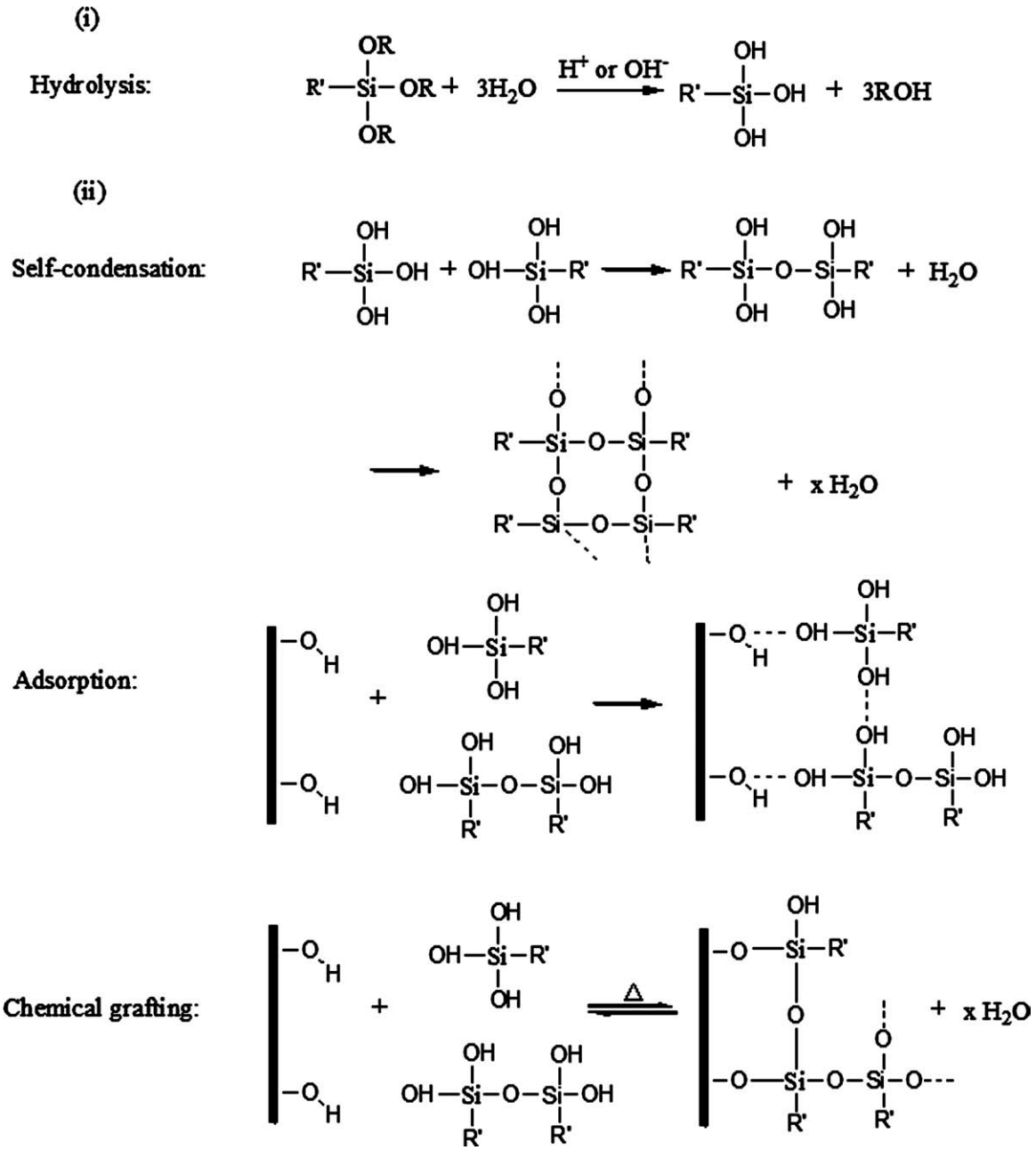

Figure 1 Interaction of silane with natural fibers by hydrolysis process.

between the filler and matrix. It improves the interfacial adhesion when one end of the molecule is tethered to the filler surface and the functionality at the other end reacts with the polymer phase.

Interaction of silane coupling agents with natural fibers likely proceeds through two steps.[13] First, the silane monomers are hydrolyzed liberating alcohol and yielding reactive silanol groups. Second, the silanol groups and natural fibers undergo self-condensation, adsorption, and chemical grafting as illustrated in Figure 1, chemical grafting is especially beneficial for the cross-linking of the fiber cell walls.

Varieties of silanes (mostly trialkoxysilanes) have been applied as coupling agents in natural fiber composites to promote interfacial adhesion and improve the properties of composites. The interaction mechanism between the silane-treated fibers and the polymer matrices is a crucial factor. Physical blending of the silane-treated natural fibers and the thermoplastic polymers enhances their mutual adherence via inter-molecular entanglement or acid–base interactions. In the case of aminosilanes, the amino groups cannot react with the hydrocarbon backbone of polypropylene or polyethylene, but the natural fibers and thermoplastic polymers treated with APS were reported to provide somewhat better mechanical properties than untreated ones.[14] Acid–base interfacial adhesion was also reported for

TABLE I
The Silane Coupling Agents and Their Chemical Structures

Silane	Chemical names	Chemical structures
AEAPTES	3-(2-Aminoethylaminopropyl)-triethoxysilane	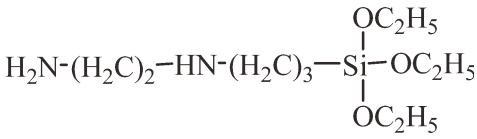
AEAPTMES	3-(2-Aminoethylaminopropyl)-trimethoxysilane	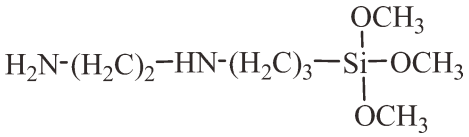
APTES	3-Aminopropyltriethoxysilane	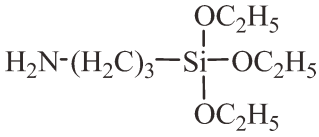
APTMES	3-Aminopropyltrimethoxysilane	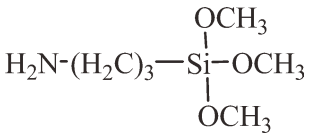

composites composed of the aminosilane-treated fibers and specific thermoplastic polymers with acidic or basic characteristics, e.g., polystyrene and polyvinyl chloride.[15,16]

This research studied the effect of the interaction mechanism between aminosilane-treated rice straw fiber (TRSF) and poly(butylenes succinate) PBS. TRSF-PBS composites were prepared by TRSF with four silane coupling agents: 3-aminopropyltriethoxysilane (APTES), 3-aminopropyltrimethoxysilane (APTMES), 3-(2-aminoethylaminopropyl)-triethoxysilane (AEAPTES), and 3-(2-aminoethylaminopropyl)-trimethoxysilane (AEAPTMES). In addition, the effect of the alkoxy groups of the aminosilanes was also studied.

EXPERIMENTAL SECTION

Materials

PBS is completely biodegradable polyester with good mechanical properties and thermal stability; it was chosen as the matrix (PBS 1020, Showa High Polymer) and has a density of 1.26 g/cm^3, a melting point of 115°C.

RSF was obtained from a local farm. After crushing the fibers, they were sieved and classified into three groups: under 106 μm, 106–300 μm and 300–1000 μm. Their average aspect ratios were about 1.2, 3.7, and 5.8, respectively.

The aminosilane coupling agents (APTES, APTMES, AEAPTES, and AEAPTMES) were supplied by Yong Guang Chemical (Nanjing, China). The chemical structures and description were listed in Table I.

Fiber treatment

Valadez-Gonzalez et al.[17] studied the deposition of silane on the surface of natural fiber in aqueous silane solution by a typical adsorption experiment, the absorbed silane was measured from the change of silane concentration in the solution before and after the absorption, only low contents of silane are observed in the final treated fibers. In contrast, dry blending with silane is beneficial to get a higher amount. In this study, the RSF was dry-blended with each of the four aminosilane coupling agents in a stirrer (T-626, Unicom) for 3 min. Then the fiber mixture was dried at 80°C for 24 h.

Specimen preparation

The RSF-PBS and TRSF-PBS composites with the desired fiber weight content (10, 20, 30 wt%) were prepared by injection molding. These mixtures were formed into specimens using an injection molding machine (NP7-1F, Nissei Plastic Industrial, Nagano, Japan); The temperature profile used was 50–160°C from feed to die (50, 120, 130, 140, 150, 160°C), the molding temperature was 40°C, cooling time was 30 s, injection pressure was 90 MPa, and injection rate was 52.8 mm/s. The dumbbell-shaped specimens (parallel body, length × width × thickness of

30 mm × 5 mm × 2 mm) were prepared to perform the tensile test according to JIS K7113 1 (1/2); the rectangular specimens (80 mm × 10 mm × 2 mm, length × width × thickness) were prepared to perform the water absorption test. The results of tensile and water absorption test were calculated as the arithmetic mean of measurements from five and three specimens, respectively.

Fourier transforms infrared spectroscopy

The infrared spectra were measured using a micro sampling FTIR spectrometer (MFT-2000, Jasco, Tokyo, Japan) with the KBr pellet method. Between 4000 and 600 cm^{-1} the resolution was 4 cm^{-1}. Fifty scans were averaged for each sample.

Surface electric charge of (T)RSF

The ζ potential was utilized for the surface charge study of the untreated and treated RSF. The ζ potential was determined in a 0.001*M* KCl electrolyte solution using a ζ potential analyzer (Zetaplus, Brookhaven Instruments Corporation, NY, America).

X-ray diffraction

X-ray diffraction (XRD) patterns were recorded in the range of $2\theta = 5$–90° by step scanning with a diffractometer (XRD-6000, Shimadzu, Kyoto, Japan). Nickel-filter Cu Kα radiation ($\lambda = 0.15417$ nm) was used with a generator voltage of 40 kV and a current of 30 mA. The crystallinity index (CrI) of the RSF was calculated according to the Segal empirical method as follows[18–19]:

$$\mathrm{CrI}(\%) = (I_{002} - I_{\mathrm{am}})/I_{002} \times 100 \quad (1)$$

where I_{002} is the maximum intensity of the 002 lattice reflection of the cellulose crystallographic at 2θ angles of 22° and 23° and I_{am} is the intensity of diffraction of the amorphous material, which is taken at a 2θ angle between 18° and 19° when the intensity is minimum.

Mechanical properties

Tensile testing was carried out using dumbbell-shaped specimens according to JIS K7113 on a universal testing machine (Series 3360, Instron, Canton, America) at a crosshead displacement rate of 10 mm/min.

Morphological investigations

Morphology of the fractured specimens after tensile testing was observed. Dispersion of RSF and interfacial adhesion between RSF and PBS were examined using a scanning electron microscope (S-4300, Hitachi, Tokyo, Japan). The fracture surface was sputter-coated with gold to provide enhanced conductivity.

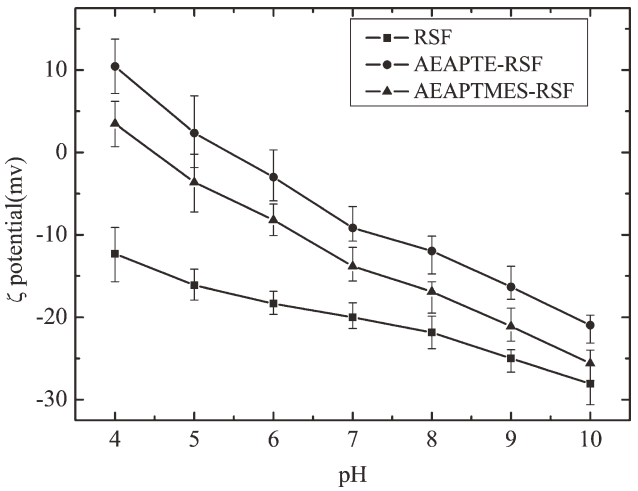

Figure 2 ζ potential versus pH of RSF, AEAPTES-RSF, and AEAPTMES-RSF.

Water absorption test

The rectangular specimens were used to examine water absorption behavior after vacuum drying at 60°C for 24 h. Three specimens of every sample were immersed in distilled water (25°C) and periodically taken out of the water, the excess water on the surface was removed by blotting with tissue paper and specimens were weighed. The amount of water absorbed (M_t) was calculated as follows:

$$M_t(\%) = (W_r - W_0)/W_0 \quad (2)$$

where W_t and W_0, are the weights of the specimen before and after immersion in water, respectively.

RESULTS AND DISCUSSION

Surface electric charge determined by ζ potential

The surface treatment of natural fibers can be measured by the electrokinetic method. The ζ potentials of RSF, AEAPTES-RSF, and AEAPTMES-RSF were shown in Figure 2. RSF displayed an acidic character because of the negative ζ potential: the negative ζ potential increase with increasing pH was caused by the enhanced adsorption of hydroxyl ions.[20] After silane treatment, the aminosilane introduced amino groups which shift the isoelectric point (where $\zeta = 0$) of TRSF toward the alkaline range, at low pH the ζ potential was positive due to the protonation of the amino groups. It was noteworthy that the ζ potential of AEAPTES-RSF was higher than AEAPTMES-RSF although AEAPTMES had higher levels of amino groups (13.94%) than AEAPTES (11.74%). This implied more hydroxyl ions were grafted onto the

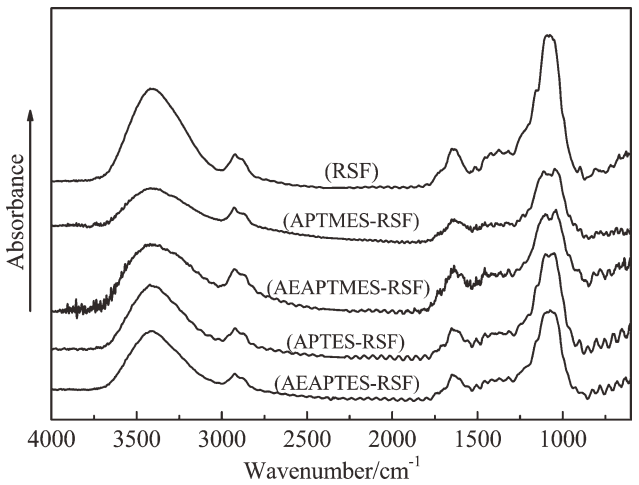

Figure 3 FTIR spectra of RSF and TRSF.

fiber surface by silane hydroxyl with AEAPTES, and the silanol formation of AEAPTMES was mostly due to self-condensation, not chemical grafting. This might be because the relative rates of hydrolysis and ensuing silanol self-condensation of methoxy silane were too fast to reduce the number of silanol groups grafted on the fiber surface.

FTIR analysis

To investigate the effect of silane coupling agents on RSF, FTIR spectra of RSF, and TRSF were measured and the results were presented in Figure 3. The RSF spectrum had a broad absorption band characteristic of OH groups: the O—H stretching and intermolecular hydrogen bond of OH···O, from 3600 to 3200 cm^{-1}. The strong band around 1100 cm^{-1} is attributed to the glycosidic bond vibration (C—O—C) overlapped with stretching vibrations of C—OH in cellulose, hemicelluloses, and lignin (C—O—C stretching at 1000–1160 cm^{-1}, C—O stretching of the primary hydroxyl group at 1000–1060 cm^{-1}, C—O stretching of the secondary hydroxyl group at 1070–1120 cm^{-1}, and C—O stretching of the tertiary hydroxyl group at 1050–1160 cm^{-1}).[21,22] After silane treatment, there was an obvious peak split around 1100 cm^{-1} for AEAPTMES-RSF and APTMES-RSF, the new peak which occurs at the lower wave number was attributed to the Si—O—Si stretching[23]; interestingly, the Si—O—Si peak in APTES-RSF was very weak and almost could not be seen in AEAPTES-RSF. This might suggest more hydroxyl groups of RSF were chemically grafted, thus Si—O—C overlapped the peak of C—O—C and Si—O—Si which accords with the ζ potentials analysis.

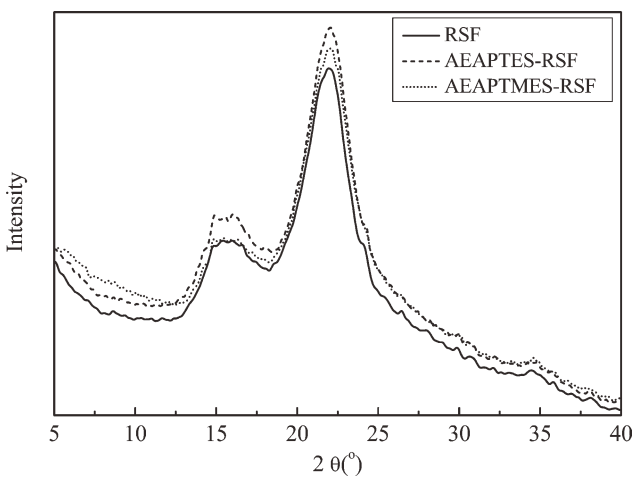

Figure 4 X-ray diffraction patterns of RSF and TRSF.

TABLE II
Crystallinity Indices of Untreated and Treated RSF

Sample	CrI (%)
RSF	45.65
AEAPTES-RSF	45.99
AEAPTMES-RSF	45.72
APTES-RSF	46.18
APTMES-RSF	46.25

XRD examination of (T)RSF

Since the chemical treatment might influence the crystallinity of natural fibers,[3,24] the influence of silane treatment was examined from the X-ray diffraction patterns of RSF and TRSF which were given in Figure 4. Their patterns exhibited distinct peaks at $2\theta = 16°$, 22°, and 34.5°. The 16° reflection corresponds to crystallographic planes (110). The respective peaks at $2\theta = 22$ and 34.5 indicated respectively the (002) and (023) crystallinity planes.[24]

The CrI of RSF and TRSF was calculated according to the Segal empirical method described in the experimental section and the results were presented in Table II. The CrI of TRSF was not significantly

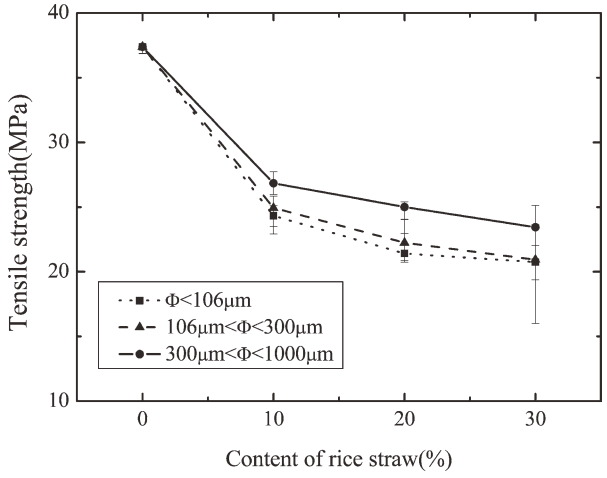

Figure 5 Effect of RSF content and particle size on tensile strength.

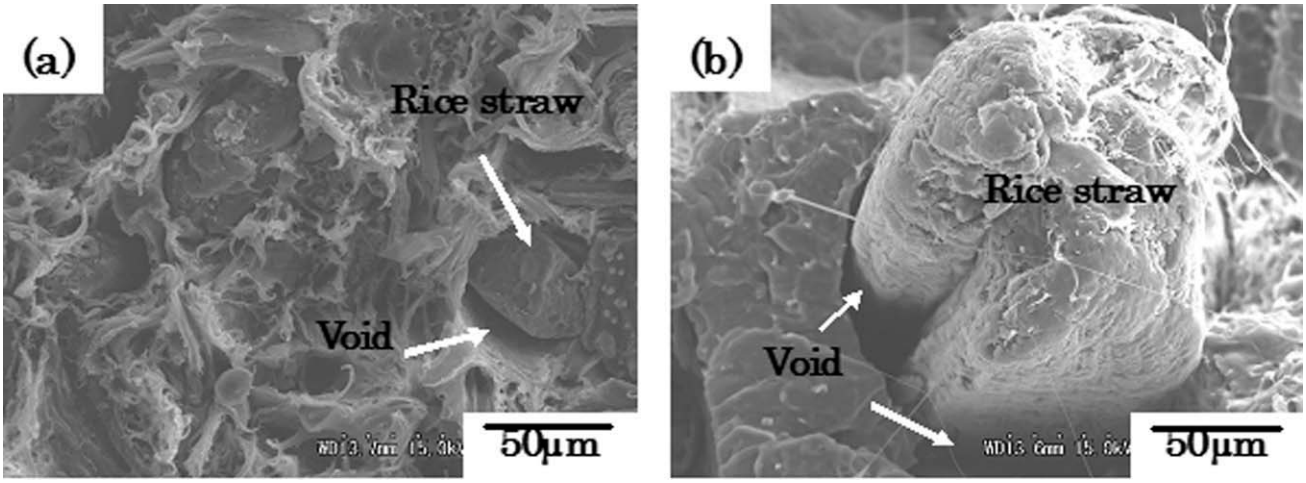

Figure 6 SEM micrographs of RSF-PBS (30/70 w/w) composites with particle size of (a) Φ <106 μm and (b) 300 < Φ < 1000 μm.

affected by the silane treatment, this might be because the spraying only results in a surface coating with silanes, the polysiloxane layer on the fiber surface may hinder diffusion of the silane molecules into the cell wall, or result in a concentration gradient in the cell walls. Thus the silanol could not diffuse into the crystalline region of the cellulose.

Tensile properties

The effect of untreated RSF loading on tensile properties and interfacial morphology

Figure 5 showed the effect of RSF content and particle size on the tensile properties of RSF-PBS composites without silane treatment, the tensile strength gradually decreased with the increase of RSF content for different particle size, this might be due to poor interfacial adhesion between the polymer matrix and RSF filler. This was a general phenomenon in incompatible composites with different characteristics.[25,26] It should be pointed out that after 10% RSF was added, the tensile strength of composites decreases ~ 30% compared with pure PBS. When the amount of RSF filler continues to increase, the decrease of the tensile strength was only several percent till the RSF content reaches 30 wt %. This means that significant amount of RSF could be added to reduce the total material costs. And at the same RSF content, with larger particle size, the higher tensile strength was gotten, because the relatively high aspect ratio of filling was favorable for reinforcement composites.[27,28]

Figure 6 showed the SEM micrographs of the fracture surface of the RSF-PBS (30 g/70 g) composites (particle size of RSF: <106 μm and 300–1000 μm), two phases could be seen clearly; also large voids between RSF and PBS matrix were visible. These findings suggested that the interaction between RSF and PBS was very weak, resulting in less interfacial adhesion, which was a typical of incompatible polymer composites. In Figure 6(a) many more fibers were pulled out from the matrix in the fracture process, compared to Figure 6(b), which confirmed that larger particle size was beneficial.

The effect of silane treatment on tensile properties and interfacial morphology

The effect of the four silane coupling agents on the tensile properties of the RSF-PBS composites (30/70 w/w, 100–300 μm) was investigated and results were indicated in Figure 7. The tensile strength of composites which were treated with AEAPTES and APTES increases sharply at first with increasing amount of silane; when excess silane was added, the tensile strength of the composite begins to decrease,

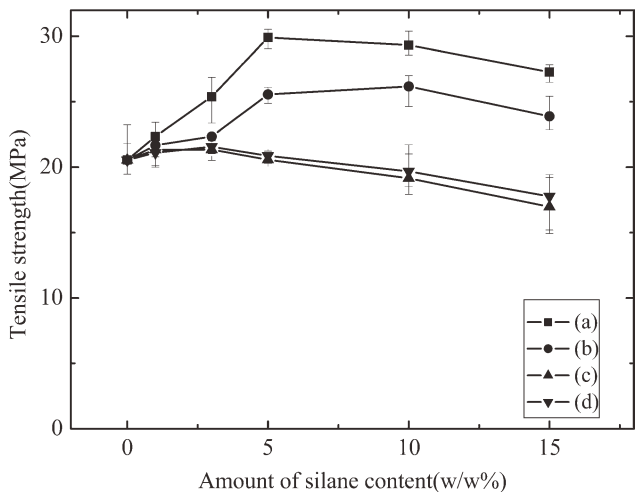

Figure 7 Effect of silane content on the tensile properties of (T)RSF-PBS composites (30/70 w/w, 100–300 μm): (a) AEAPTES, (b) APTES, (c) AEAPTMES, and (d) APTMES.

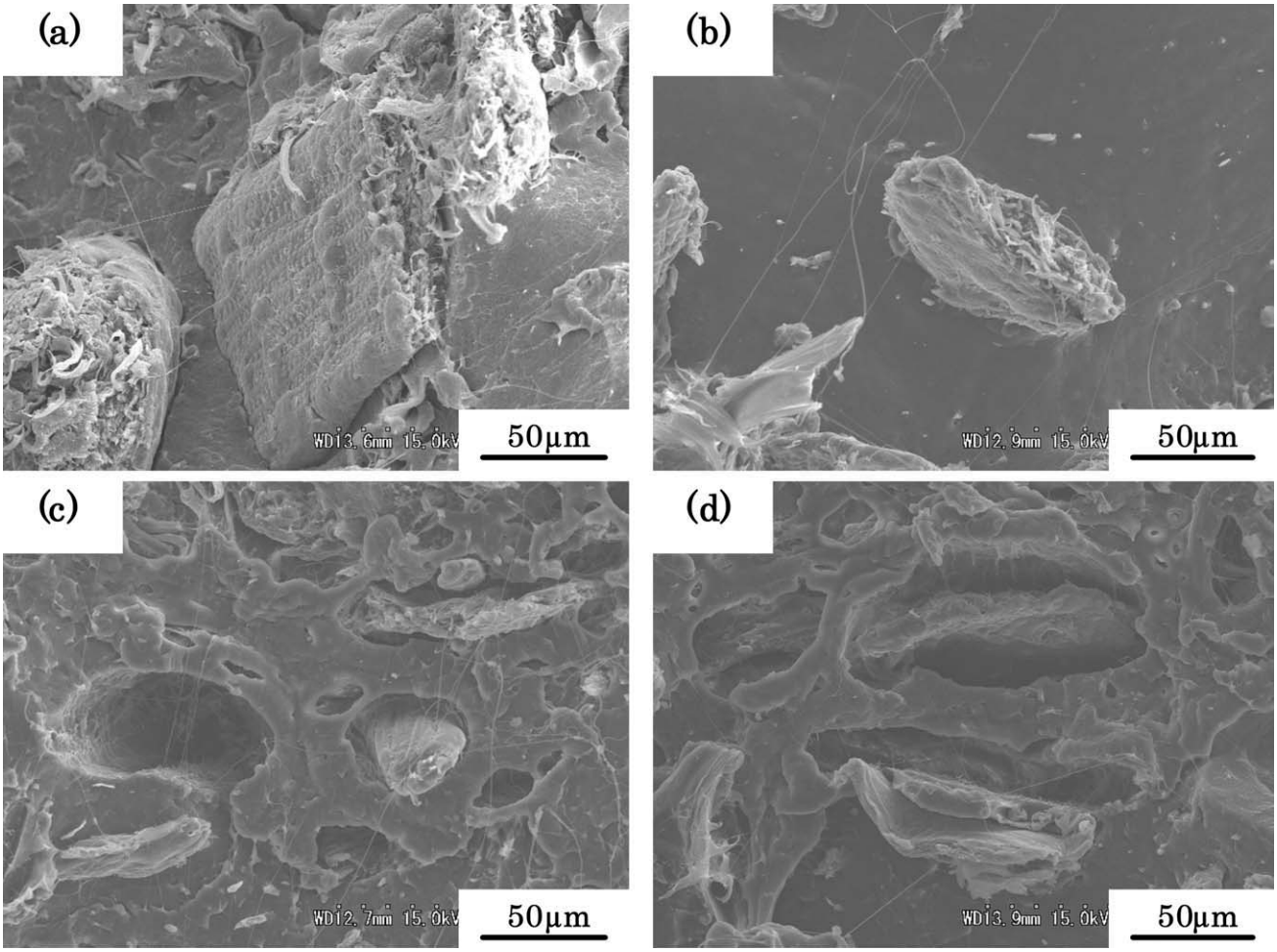

Figure 8 SEM micrographs of 5 wt % silane-treated RSF-PBS composites (30/70 w/w, 100–300 μm): (a) AEAPTES (b) APTES (c) AEAPTMES, and (d) APTMES.

and the silane amount at which the tensile strength reached a plateau could be considered the critical interfacial concentration, which was the minimum value of interfacial saturation for a coupling agent in the dispersed phase.[29–31] The tensile strength of composites obtained by using AEAPTMES and APTMES almost did not change. It was noteworthy that AEAPTMES and APTMES were methoxy silanes, and the silane treatment might not work because too many silanol groups underwent self-condensation, rather than chemical grafting on the RSF which according with conclusions drawn from the FTIR and ζ potential measurements.

Tensile properties of composites will be affected by their morphology. Figure 8 showed SEM micrographs of the tensile fractured surface of TRSF-PBS composite. From Figure 8(a,b), it was seen that a more uniform interface between TRSF and PBS was obtained which was considered to be the reason for the tensile strength increased.[32] From Figure 8(c,d), voids could be seen between fibers and PBS matrix; they indicated poor adhesion between TRSF and PBS matrix.

Figure 9 showed the effect of RSF particle size on AEAPTES treated RSF-PBS composites (30/70 w/w). It could be seen that the tensile strength gradually

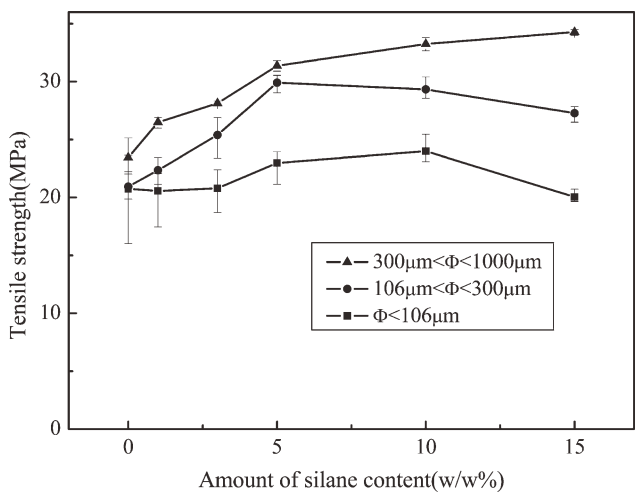

Figure 9 Effect of RSF particle size on the tensile properties of AEAPTES-RSF-PBS composites (30% w/w fiber loading).

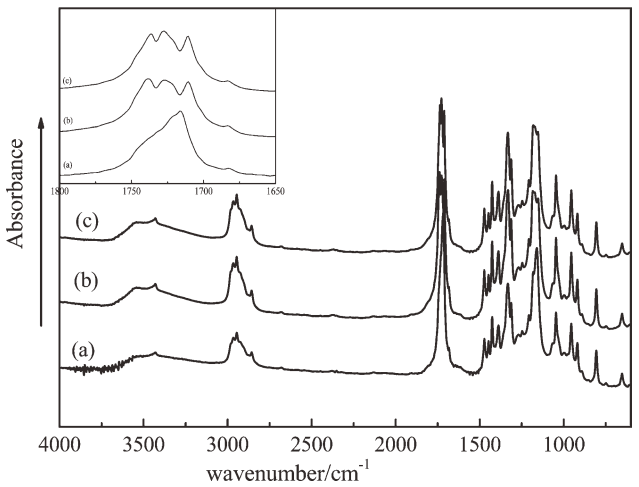

Figure 10 FTIR spectra of: (a) RSF-PBS (b) AEAPTES-RSF-PBS, and (c) AEAPTMES-RSF-PBS.

increased with the increasing of AEAPTES content for different particle sizes of RSF. The tensile strength began to decrease when excess silane was added. The critical content was not exactly the same. And at the same RSF content, with larger particle size, the higher tensile strength was higher. This was because of the relatively high aspect ratio accords with the results of Figure 5.

Study of the mechanism between aminosilane-treated RSF and PBS

FTIR was preformed to investigate the mechanism between TRSF and PBS. Figure 10 showed the FTIR spectra of RSF-PBS, AEAPTES-RSF-PBS, and AEAPTMES-RSF-PBS, the stretching band of RSF-PBS at $\sim$ 1715 cm^{-1} was assigned to the carbonyl groups of PBS, while the bands at 1722 and 1731 cm^{-1} were attributed to hydrogen-bonded carbonyl groups,[33–38] the formation of which caused a blue-shift.[39] The peaks occurring at different locations were assigned to hydrogen-bonds and double contract hydrogen-bonds.[40–41] Therefore the results indicated that the surface amine of AEAPTES- and AEAPTMES-treated RSF attack the PBS polymer through the hydrogen-bonds and thus increased the interfacial adhesion. The weak tensile strength between AEAPTMES-RSF and PBS might be because the AEAPTMES undergoes mostly self-condensation, not chemical grafting on RSF which according with the findings from the FTIR and ζ potential measurements.

Water absorption

Figure 11 showed the water absorption curves of PBS and (T)RSF-PBS (30/70 w/w, 100–300 μm) composites. Pure PBS showed low water absorption because of its hydrophobicity. However, the water absorption of RSF-PBS significantly increased; the hydrophilic character of natural fibers was responsible for the water absorption in the composites, and therefore a higher content on fibers leads to a higher amount of water absorbed as shown in Table III. The treatment of RSF by aminosilane decreased the water uptake compared with untreated RSF-PBS composites, and the decrease due to the ethoxy silane treatment was more than that for the methoxy silane treatment which indicated the reactive hydrophilic hydroxyl groups of the RSF were chemical grafted by the silanol of the ethoxy silane.

Water penetration into composite materials might occur by three different mechanisms. The main process consisted of diffusion of water molecules inside the micro gaps between polymer chains. The other common mechanisms were capillary transport into the gaps and flawed at the interfaces between the fillers and polymer matrices, because of incomplete wettability and impregnation; and transport through matrix microcracks, which were formed during the compounding process.[42,43] In spite of the fact all three mechanisms were jointly active in the composite materials; the overall effect could be modeled conveniently considering only the diffusion mechanism.

In general, the diffusion behavior in polymers could be classified according to the relative mobility of the penetrant and of the polymer segments. With this, there were three different categories of diffusion behavior.[43]

Case I (Fickian diffusion), in which the rate of diffusion is much less than that of the polymer segment mobility. The equilibrium inside the polymer is rapidly reached and it is maintained independently time.

Case II, in which penetrant mobility is much greater than other relaxation processes. This diffusion is characterized by the development of a

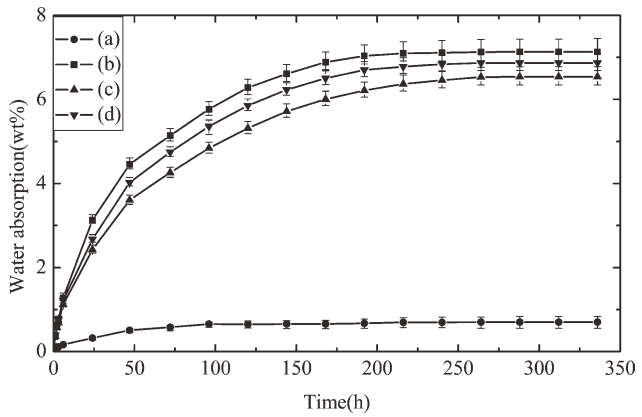

Figure 11 Water absorption curves of PBS and (T)RSF-PBS composite (30/70 w/w, 100–300 μm): (a) PBS, (b) RSF-PBS, (c) 3 wt % AEAPTES-RSF-PBS, and (d) 3 wt % AEAPTMES-RSF-PBS.

TABLE III
Values of Water Absorption at Saturation, Diffusion Case Selection Parameters, and Diffusion Coefficient (*D*)

RSF (μm)	Sample w/w	Water absorption (%)	*n*	*k*	*D* ($cm^2/s \times 10^{-12}$)
Φ<106	RSF-PBS(10/90)	1.92	0.45397	0.09823	2.35
	RSF-PBS(20/80)	2.42	0.47248	0.08742	2.04
	RSF-PBS(30/70)	6.46	0.52952	0.06219	2.21
	RSF-PBS(30/70) 3%AEAPTES	5.68	0.53386	0.06632	1.76
	RSF-PBS(30/70) 3%AEAPTMES	5.66	0.54281	0.07823	1.82
	RSF-PBS(30/70) 3%APTES	5.82	0.52188	0.08227	1.88
	RSF-PBS(30/70) 3%APATMES	5.79	0.53169	0.08698	1.86
106<Φ<300	RSF-PBS(10/90)	2.41	0.47204	0.08942	2.24
	RSF-PBS(20/80)	3.84	0.51667	0.06737	1.52
	RSF-PBS(30/70)	7.13	0.55337	005944	1.96
	RSF-PBS(30/70) 3%AEAPTES	6.54	0.52651	0.06516	1.41
	RSF-PBS(30/70) 3%AEAPTMES	6.78	0.54233	0.0736	1.47
	RSF-PBS(30/70) 3%APTES	6.82	0.53496	0.06382	1.51
	RSF-PBS(30/70) 3%APATMES	6.87	0.55485	0.07884	1.54
300<Φ<1000	RSF-PBS(10/90)	3.19	0.47365	0.08661	2.11
	RSF-PBS(20/80)	5.76	0.47296	0.0868	1.89
	RSF-PBS(30/70)	7.62	0.48953	0.08106	2.11
	RSF-PBS(30/70) 3%AEAPTES	7.02	0.56269	0.06559	1.25
	RSF-PBS(30/70) 3%AEAPTMES	7.16	0.53728	0.07112	1.33
	RSF-PBS(30/70) 3%APTES	7.52	0.54265	0.07968	1.48
	RSF-PBS(30/70) 3%APATMES	7.48	0.55632	0.08223	1.54

boundary between the swollen outer part and the inner glassy core of the polymer. The boundary advances at a constant velocity and the core diminishes in size until an equilibrium penetrant concentration is reached in the whole polymer.

Case III (Non-Fickian or anomalous diffusion), in which occurs when the penetrant mobility and the polymer segment relaxation are comparable. It is then, an intermediate behavior between Cases I and II.

These three cases of diffusion can be distinguished theoretically by the following equation[44]:

$$\lg\left(\frac{M_t}{M_\infty}\right) = \lg(k) + n\lg(t) \tag{3}$$

Where M_t is the water absorption at time t; M_∞ is the water absorption at equilibrium; and k and n are constants. The value of n differs between cases; for Fickian diffusion $n = 1/2$; while for Case II $n = 1$. For anomalous diffusion, n shows an intermediate value ($1/2 < n < 1$).

Figure 12 showed an example fitting the experimental date to eq. (3). In Table III, the parameters n and k resulting from the fitting were shown for absorption specimens. The values of n were very similar for all the specimens and close to $n = 0.5$ which indicated that water absorption of (T)RSF-PBS composites approaches the Fickian diffusion case. Aminosilane did not change the mechanism of water adsorption.

Next step is the performance of an analysis of the parameters of this theoretical model. The diffusion coefficient (D) is the most important parameter of the Fick's model, as this shows ability of solvent molecules to penetrate inside the composite structure. For small times ($M_t/M_\infty \leq 0:5$), the following equation can be used

$$\frac{M_t}{M_\infty} = \frac{4}{L}\left(\frac{D}{\pi}\right)^{0.5} t^{0.5} \tag{4}$$

where L is the thickness of the sample.

By eq. (4), the moisture diffusion coefficient could be obtained from the slope of the linear part of the plot of M_t/M_∞ vs. $(\text{time})^{0:5}L^{-1}$; the moisture diffusion coefficient obtained from the fitting of the linear part was also presented in Table III.

From the results as shown in Table III, it was evident that the diffusion coefficients firstly decreased with RSF content increase from 10 to 20 wt % and

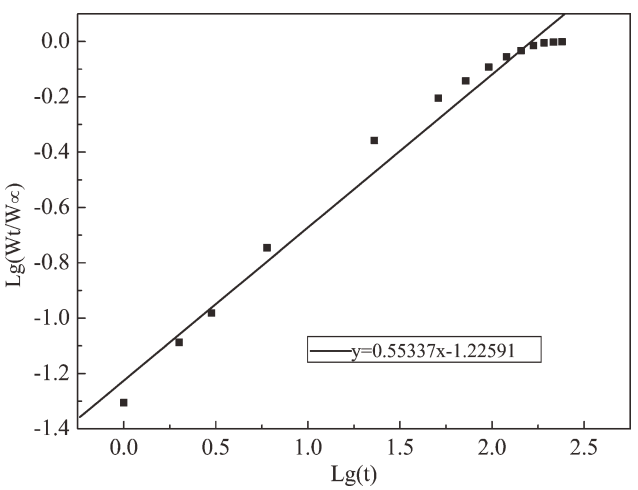

Figure 12 Diffusion case fitting plots for RSF/PBS composites (30/70 w/w, 100–300 μm).

then increased with more RSF was blended. An explanation of this behavior should be necessary because the high hygroscopicity of RSF falsely leads one to expect also high diffusion coefficient. However, RSF is a hygroscopic material; the dry RSF in the composites therefore represents a potential energy "sink" than can attract and bind water molecules and thus limited the diffusion of water molecules. When more RSF was added, the diffusion coefficient would rapidly increase because the connectivity of the RSF. Crank had discussed the diffusion in laminate systems that have a "skin" of one component on the surface.[45] When the diffusion coefficient of the inner component is greater than that of the skin, the sorption curve has a parabolic shape. Few authors had also reported this behavior.[44,46]

The aminosilane treatment significantly reduced the moisture diffusion coefficient, this was might because of the H-bonding between TRSF and polymer matrix retards the diffusion of the water molecules and increases the activation energy of diffusion.[47]

CONCLUSIONS

AEAPTES was observed to be a suitable adhesion promoter for RSF-PBS composites, significantly improving the tensile strength of the composites and the interaction between RSF and PBS matrix. FTIR spectroscopy results suggested that aminosilane could form hydrogen-bonds with the ester carbonyl of the PBS matrix, thus improving the tensile strength. This might provide a new perspective for investigating compose filling with polymer containing ester carbonyl. Ethoxy silane treatment of the TSF was more effective than methoxy silane treatment because ethoxy silane led to more efficient chemical grafting on RSF. Water absorption of (T)RSF-PBS composites was described by Fickian diffusion. The aminosilane treatment significantly reduced the moisture diffusion coefficient but did not change the mechanism of water adsorption.

This research was supported by the Environment Research and Technology Development Fund (K113018) of the Ministry of the Environment, Japan.

References

1. Joshi, S. V.; Drzal, L. T.; Mohanty, A. K.; Arora, S. Compos Part A 2004, 35, 371.
2. Hill, C. A. S.; Khalil, H. P. S. A. J Appl Polym Sci 2000, 78, 1685.
3. Zhao, Y., Qiu, J. H.; Feng, H. X.; Zhang, M.; Lei, L.; Wu, X. L. Chem Eng J 2011, 173–659.
4. Pfister, D. P.; Larock, R. C. Compos Part A 2010, 41, 1279.
5. Takagi, H.; Asano, A. Compos Part A 2008, 39, 685.
6. George, J.; Sreekala, M. S.; Thomas, S. Polym Eng Sci 2001, 41, 1471.
7. Shibata, S.; Cao, Y.; Fukumoto, I. Compos Part A 2008, 39, 640.
8. Qin, L. J.; Qiu, J. H.; Liu, M. Z.; Ding, S. L.; Shao, L.; Lu, S. Y.; Zhang, G. H.; Zhao, Y.; Fu, X. Chem Eng J 2011, 166, 772.
9. Raj, R. G.; Kokta, B. V.; Dembele, F.; Sanschagrain, B. J Appl Polym Sci 1989, 38, 1987.
10. Kazayawoko, M.; Balatinecz, J. J.; Matuana, L. M. J Mater Sci 1999, 34, 6189.
11. Bisanda, E. T. N.; Ansell, M. P. Compos Sci Technol 1991, 41, 165.
12. Singh, B.; Gupta, M.; Verma, A. Polym Compos 1996, 17, 910.
13. Arkles, B.; Steinmetz, J. R.; Zazyczny, J.; Mehta, P. J Adhes Sci Techno 1992, l6, 193.
14. Matuana, L. M.; Woodhams, R. T.; Balatinecz, J. J.; Park, C. B. Polym Compos 1998, 19, 446.
15. George, J.; Bhagawan, S. S.; Thomas, S. J. Therm Anal 1996, 47, 1121.
16. Laly, A. P.; Sabu, T. Compos Sci Technol 2003, 63, 1231.
17. Valadez-Gonzalez, A.; Cervantes-Uc, J. M.; Olayo, R.; Herrera-Franco, P. J. Compos Part B 1999, 30, 321.
18. Tserki, V.; Zafeiropoulos, N. E.; Simon, F.; Panayiotou, C. Compos Part A 2005, 36, 1110.
19. Zafeiropoulos, N. E.; Williams, D. R.; Baillie, C. A.; Matthews, F. L. Compos Part A 2002, 33, 1083.
20. Bellmann, C.; Caspari, A.; Albrecht, V.; Doan, T. T. L.; Mader, E.; Luxbacher, T.; Kohl, R. Colloid Surf A 2005, 267, 19.
21. Rana, A. K.; Basak, R. K.; Mitra, B. C.; Lawther, M.; Banerjee, A. N. J Appl Polym Sci 1997, 64, 1517.
22. Fu, P.; Hu, S.; Xiang, J.; Sun, L.S.; Yang, T.; Zhang, A. C.; Zhang, J. J. Chin J Chem Eng 2009, 17, 522.
23. Anirudhan, T. S.; Tharun, A. R.; Rejeena, S. R. Ind Eng Chem Res 2011, 50, 1866.
24. Zafeiropoulos, N. E.; Williams, D. R.; Baillie, C. A.; Matthews, F. L. Compos Part A 2002, 33, 1083.
25. Sain, M. M.; Kokata, B. V.; Maldas, D. J Adhes Sci Technol 1993, 7, 49.
26. Xu, B.; Simonsen, L.; Rochefort, W. E. J Appl Polym Sci 2001, 79, 418.
27. Quijano-Solis, C.; Yan, N.; Zhang, S. Y. Compos Part A 2009, 40, 351.
28. Jiang, B.; Liu, C.; Zhang, C.; Wang, B.; Wang, Z. Compos Part B 2007, 38, 24.
29. Liu, W.; Wang, Y. J.; Sun, Z. J Appl Polym Sci 2003, 88, 2904.
30. Lacasse, C.; Favis, B. D. Adv Polym Technol 1999, 18, 255.
31. Liang, H.; Favis, B. D.; Yu, Y. S.; Eisenberg, A. Macromolecules 1999, 32, 1637.
32. Alvarez, V. A.; Terenzi, A.; Kenny, J. M.; Vázquez, A. Polym Eng Sci 2004, 44, 1907.
33. Coleman, M. M.; Pehlert, G. J.; Painter, P. C. Macromolecules 1996, 29, 6820.
34. Hong, J.; Goh, S. H.; Lee, S. Y.; Siow, K. S. Polymer 1995, 36, 143.
35. Hu, Y.; Painter, P. C.; Coleman, M. M. Macromolecules 1998, 31, 3394.
36. Pehlert, G. J.; Painter, P. C.; Vetysman, B.; Coleman, M. M. Macromolecules 1997, 30, 3671.
37. Pehlert, G. J.; Painter, P. C.; Coleman, M. M.; Macromolecules 1998, 31, 8423.
38. Tan, H.; Guo, M.; Du, R. N.; Xie, X. Y.; Li, J. H.; Zhong, Y. P.; Fu, Q. Polymer 2004, 45, 1647.
39. Keshavarz, K. M.; Cox, S. D.; Angus, R. O. J.; Wudl, F. Synthesis 1988, 20, 641.
40. Rozas, I.; Alkorta, I.; Elguero, J. J Phys Chem A 1998, 102, 9925.
41. Li, A. Y. J Phys Chem A 2006, 110, 10805.
42. Lin, Q. F.; Zhou, X. D.; Dai, G. J Appl Polym Sci 2002, 85, 2824.
43. Comyn, J. Polym Permeability 1985, 383.
44. Espert, A.; Vilaplana, F.; Karlsson, S. Compos Part A 2004, 35, 1267.
45. Crank, J. The Mathematics of Diffusion. New York: Oxford University Press, 1975.
46. Willett, J. L. Polym Eng Sci 1995, 35, 1184.
47. Park, H. S.; Sung, J.; Chang, T. Macromolecules 1996, 29, 3216.